Transactions of the Materials Research Society of Japan 28 [3] 615-618 (2003)

Fatigue Properties of a TiNi Shape-Memory Alloy Wire in Bending

Yuji Furuichi, Hisaaki Tobushi and Ryosuke Matsui
Aichi Institute of Technology, Department of Mechanical Engineering
1247 Yachigusa, Yagusa-cho, Toyota, Aichi, 470-0392 Japan
Fax: 81-565-48-4555, e-mail: tobushi@me.aitech.ac.jp

Bending-fatigue tests on a TiNi shape-memory alloy wire were performed for various strain ratios. The results obtained can be summarized as follows. (1) The fatigue life curves under alternating bending and pulsating bending, as expressed by the relationship between maximum strain and the number of cycles to failure, systematically follow the order of strain ratio. (2) The larger the strain ratio, the longer the fatigue life. (3) The fatigue life under rotating bending is shorter than that under alternating bending. (4) The fatigue limit of strain for alternating bending, pulsating bending and rotating bending is in the region of R-phase transformation.
Key words: Shape Memory Alloy, Fatigue, Bending, Strain Ratio, Fatigue Life

1. INTRODUCTION

The shape memory effect and superelasticity appear depending on temperature and stress in a shape memory alloy (SMA) [1]. Since these properties have the function of actuators, SMAs have applications as intelligent materials: using the actuator functions causes SMA elements to perform cyclic motion. In evaluating the reliability of the SMA elements, the fatigue properties of the material are the most important thing to consider. In actual applications, since the SMA elements are subjected to thermomechanical cycling, the fatigue life as depending on the thermomechanical path is complex [2, 3]. Thin wires and belts are widely used as SMA elements for the facilitation of heat transfer. One of the main deformation modes of such elements is bending. The authors studied the bending fatigue properties of a TiNi SMA wire [4~6]. Since the fatigue strength of TiNi SMA depends highly on stress ratio, the fatigue life differs depending on the mode of bending. In many SMA actuator elements, the working stroke is prescribed. The fatigue properties under strain-controlled conditions are therefore important.

In the present study, the bending fatigue properties of a TiNi SMA wire are investigated and the influence of strain ratio on the fatigue life is discussed. In order to perform the study, a machine was developed to carry out alternating bending fatigue tests on wire. In order to investigate the influence of strain ratio on the fatigue life, pulsating-bending fatigue tests were carried out. The fatigue properties under alternating bending were compared with those under rotating bending.

2. EXPERIMENTAL METHOD

2.1 Materials and specimens

The material tested was a rectilinear Ti-55.4wt%Ni SMA wire, 0.75 mm in diameter, produced by Furukawa Electric Co. Its straightness was shape-memorized through shape-memory processing. This was done by holding the wire rectilinear at 673 K for 60 min followed by cooling in the furnace. The reverse transformation finish temperature A_f was about 323 K.

2.2 Experimental apparatus

A rotating-bending fatigue test machine, a pulsating-bending fatigue test machine and a newly developed alternating-bending fatigue test machine were used for the fatigue test.

The alternating-bending fatigue test machine was designed to achieve the following goals. The bending strain on the surface of the SMA wire was to be freely prescribable in a range of 0~5 % and frequency was to be selectable in a range of 0~1000 cpm.

A schematic drawing of the manufactured machine is shown in Fig. 1. By transmitting rotation from a motor ⑤ to two cranks ⑧ located to the right and left, a specimen ① is bent cyclically from side to side. The motion is transmitted smoothly by using 8 bearings between the motor and the cranks. The bending strain of the specimen ① is varied by changing the length of grips ② and the setting position of the cranks ⑦. The frequency and the number of cycles to failure are measured by the counters.

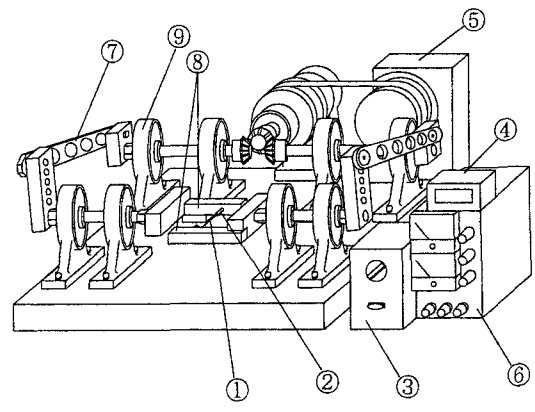

① **Specimen** ⑥ **Power source**
② **Grip** ⑦ **Crank 1**
③ **Speed controller** ⑧ **Crank 2**
④ **Counter** ⑨ **Bearing**
⑤ **Motor**

Fig1. Schematic drawing of the set up for alternating-bending fatigue test

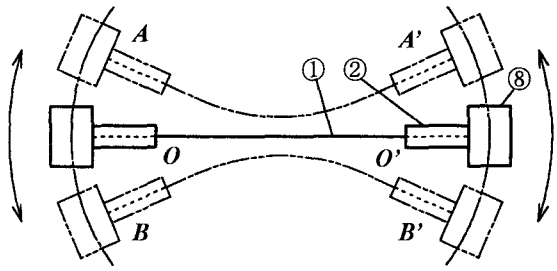

Fig.2 Grip and motion of a specimen

The state of the specimen during alternating bending is shown in Fig. 2. From the initial rectilinear state of the specimen ①, the maximum bending states AA' and BB' are applied repeatedly by the circular-arc motions AB and $A'B'$ of two cranks ⑧. Both ends of the specimen ① are held by grips ②. One end of the specimen was allowed to move freely inside a guide in one of the grips ②, while the other end remained tightly held. By means of this gripping, perfect alternating bending was achieved.

2.3 Experimental procedure

In the fatigue test, strain amplitude ε_a and strain ratio $S_r = \varepsilon_{min}/\varepsilon_{max}$ were prescribed. Three kinds of fatigue test for alternating bending ($S_r = -1$), pulsating bending ($S_r \geqq 0$) and rotating bending ($S_r = -1$) were carried out. The experiments were performed at room temperature in air. Temperature of the specimen increased during cyclic bending deformation. The temperature rise of the specimen was measured. The temperature rise of the specimen for alternating bending and pulsating bending was measured by a thermocouple and that for rotating bending by the infrared thermograph.

3. EXPERIMENTAL RESULTS AND DISCUSSION

3.1 Temperature rise during cyclic deformation

The relations of temperature rise to maximum strain ε_{max} and to frequency f, as obtained in the alternating-bending ($S_r = -1$) and pulsating-bending ($S_r = 0$) tests, are shown in Fig. 3. As can bee seen in the figure, the rate of temperature rise increases in proportion to ε_{max} and f. The areas enclosed by the hysteresis loops in the stress-strain curves denote dissipated work W_d per one cycle. In each case, W_d is proportional to the product of the MT stress σ_M and strain amplitude ε_a. Therefore, the magnitude of W_d is in proportion to ε_a, that is, to ε_{max}. Based on this assumption, temperature will rise as ε_{max} increases. Comparing the different kinds of bending, W_d in alternating bending is about twice as large as W_d in pulsating bending. Therefore temperature rise in alternating bending is about twice as large as temperature rise in pulsating bending.

3.2 Fatigue life under alternating bending and pulsating bending

The relationship between maximum strain ε_{max} and the number of cycles to failure N_f, as obtained in the fatigue tests under alternating bending and perfect pulsating bending at frequency $f = 500$ cpm, is shown in Fig. 4. As can be seen in Fig. 4, both strain-life curves display changes of direction. More precisely, the strain-life curve has a knee in the region of $\varepsilon_{max} = 0.8\sim1$ % and $N_f = (2\sim4)\times10^5$ cycles. A stress plateau due to the R-phase transformation appears in the region of strain below 0.8%, so that the R-phase transformation stress σ_R is very low at 50 MPa. Therefore the fatigue limit must be in this strain region.

Returning to Fig. 4, the fatigue life under alternating bending is shorter than that under pulsating bending. This can be explained very easily. As observed in Fig. 3, the temperature rise in alternating bending is larger than that in pulsating bending. The MT stress σ_M increases in proportion to temperature T [7], in a relationship expressed by the following equation.

$$\sigma_M = C_M(T-M_s) \qquad (1)$$

where M_s denotes the MT start temperature under no stress. The coefficient C_M of TiNi SMA is about 6 MPa/K. Therefore, if the temperature increases 10 K under cyclic bending, the MT stress will increase by 60 MPa. In the case of alternating bending, the temperature rise is large and the corresponding large increase in stress leads to a markedly greater propagation of fatigue damage, resulting in a short fatigue life.

3.3 Fatigue life in pulsating bending for various strain ratios

The relationship between maximum strain ε_{max} and the number of cycles to failure N_f, obtained from the pulsating-bending fatigue test with various strain ratios S_r at frequency $f = 500$ cpm, is shown in Fig. 5. The fatigue test was carried out for $S_r = 0$, 0.1 and 0.2. As can be seen, all the strain-life curves display changes of direction. In each case, the knee of the strain-life curve is in the region of $\varepsilon_{max} = 1\sim1.2$ % and $N_f = (2\sim4)\times10^5$ cycles. The smaller the S_r, the shorter the fatigue life. As already observed, the area enclosed by the hysteresis loop W_d for any given ε_{max} increases with each decrease in S_r. Therefore, in the case of a small S_r, the temperature rise due to W_d is large and the MT stress σ_M increases correspondingly, resulting in a short fatigue life. This relationship between a small S_r and a short fatigue life continues to hold for alternating bending ($S_r = -1$) and perfect pulsating bending ($S_r = 0$) as apparent in Fig. 4.

3.4 Formulation of low-cycle fatigue life

As discussed in the previous sections, a logarithmic graph comparing the strain-life of the SMA material with the maximum strain ε_{max} indicates that in the region of shorter fatigue life up to the knee the strain-life curve is a straight line with a constant slope.

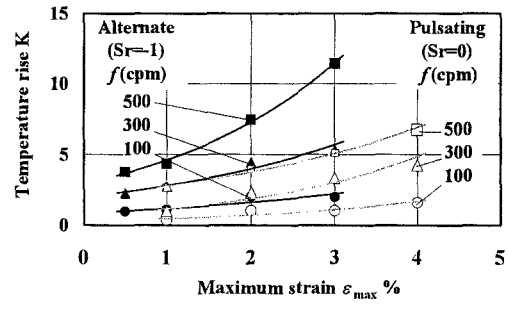

Fig.3 Relationship between temperature rise and maximum strain

As is well known, when the Manson-Coffin relationship is used to express the low-cycle fatigue life of normal metals, the fatigue life N_f is expressed by using strain amplitude ε_a as follows.

$$\varepsilon_a \cdot N_f^{\beta} = \alpha \qquad (2)$$

As apparent in Figs. 4 and 5, if the fatigue life under various strain ratios S_r is plotted against ε_{max}, the influence of S_r on the fatigue life can be expressed systematically. However, if the fatigue life is simply compared with ε_a, the influence of S_r on the fatigue life cannot be expressed systematically in this way.

The strain-life curves in the low-cycle region shown separately in Figs. 4 and 5 for alternating bending and pulsating bending are collected together in Fig. 6. Since the strain-life curve describes a straight line, this relationship can be expressed by the following equation

$$\varepsilon_{max} \cdot N_f^{b} = a \qquad (3)$$

where b and a denote the slope of the line and ε_{max} at N_f = 1, respectively. The value of b is in the region of 0.39~0.47. If a is obtained by using an average value of b, 0.42, a is almost proportional to S_r. Therefore a can be approximated by the following equation.

$$a = 1.2S_r + 2.34 \qquad (4)$$

The calculated results obtained by using Eqs. (3) and (4) are shown by the solid lines in Fig. 6. This figure shows that these calculated results match the curves of the experimental results well, and thus give a good evaluation of the low-cycle fatigue life.

3.5 Fatigue life in alternating bending and rotating bending

The relationships between strain amplitude ε_a and the number of cycles to failure N_f obtained in the alternating-bending and rotating-bending fatigue tests at frequency f= 500 cpm are shown in Fig. 7. As can be seen in this figure, both strain-life curves show a change in direction. In each case, the strain-life curve has a knee in the region of ε_a = 0.8~0.9 % and N_f = (2~4)×10^5 cycles. In the low-cycle fatigue region of $\varepsilon_a \geqq$ 1 % and $N_f \leqq 2\times10^5$ cycles, the slope of the strain-life curve is less under rotating bending and N_f in this case becomes smaller as ε_a increases. Strain ratio S_r is -1 in both rotating bending and alternating bending. The difference in fatigue life between rotating bending and alternating bending appears to be due to the difference in temperature rise, which is apparently the result of the following two causes.

The first cause is the difference in the transformed area. In the case of alternating bending, the MT occurs only in the surface area close to the lines of bending *AA'* and *BB'* in Fig. 2. On the other hand, in the case of rotating bending, the MT occurs throughout the surface area of the specimen. This means that the volume affected by MT is larger in rotating bending and therefore the heat generated is larger. This accounts for the larger temperature rise. The temperature rise under rotating bending at ε_a = 2 % and f= 500 cpm is 28 K [5]. On the other hand, the rise under the same conditions in the case of alternating bending is 7.5 K. In other words, the rise in rotating bending is about 4 times as large as that in alternating bending.

The second cause is the mechanical difference in the motion of the specimen. During rotating bending, the configuration of the bent specimen is kept constant and the

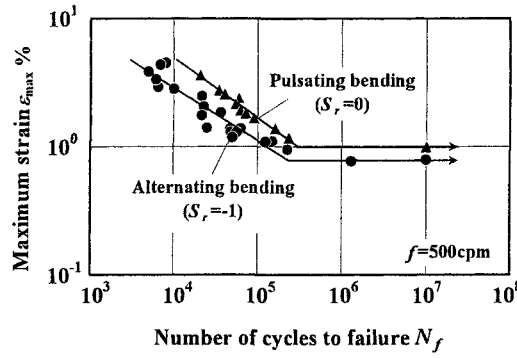

Fig.4 Relationship between maximum strain and the number of cycles to failure for alternating bending and pulsating bending

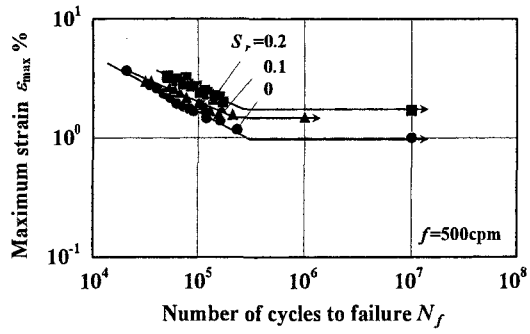

Fig.5 Relationship between maximum strain and the number of cycles to failure for pulsating bending at various strain ratios S_r

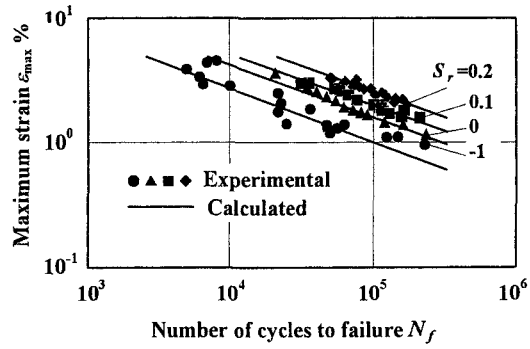

Fig.6 Strain-life curves of low-cycle bending fatigue at various strain ratios S_r

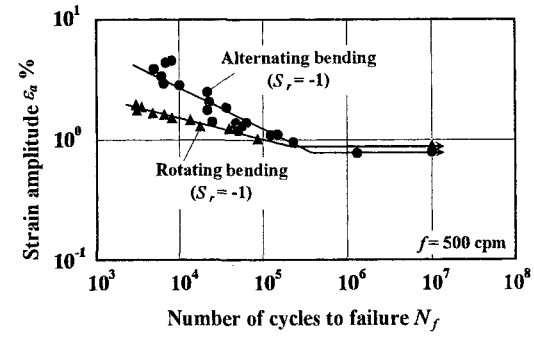

Fig.7 Relationship between strain amplitude and the number of cycles to failure for alternating bending and rotating bending

only motion is rotation. Therefore the coefficient of heat transfer between the specimen and the air is small and heat radiation into the air is limited, resulting in only a slight cooling effect. On the other hand, in alternating bending the specimen undergoes an alternate motion of bending and unbending, as shown in Fig. 2. In the case of forced-convection heat transfer around a column, the Nusselt number N_u used to represent the magnitude of heat transfer is expressed by a power function of a Reynolds number R_e. N_u depends on the velocity of the surface part of the specimen, and compared with the value for rotating bending, N_u in alternating bending is about 4 times as large. Therefore the amount of heat radiated into the air due to the motion of the specimen in alternating bending is larger. This of course results in more rapid cooling of the specimen.

For the above-mentioned two causes, the temperature rise in rotating bending is larger than that in alternating bending. This in turn leads to a greater increase in MT stress in the case of rotating bending, resulting in a shorter fatigue life.

In the R-phase transformation region of $\varepsilon_a < 1$ %, the temperature rise in the specimen subjected to cyclic bending is very small. Therefore, in this region, N_f increases markedly in both rotating bending and alternating bending, and the difference in N_f between the two kinds of bending becomes small. The difference in fatigue life in this region and the details of the behavior at the fatigue limit will be discussed in a subsequent companion paper.

4. CONCLUSIONS

In order to investigate the fatigue properties of a TiNi SMA wire, an alternating-bending fatigue test machine operated under strain-controlled conditions was developed. The bending fatigue tests were performed for various strain ratios. The results obtained can be summarized as follows.

(1) The strain-life curves with various strain ratios can be expressed systematically in relation to maximum strain.

(2) Comparing strain-life curves with maximum strain in both alternating bending and pulsating bending, the larger the strain ratio, the longer the fatigue life.

(3) In the case of alternating bending and rotating bending with a strain ratio of -1, the fatigue life under rotating bending is shorter than that under alternating bending.

(4) The temperature rise during cyclic bending increases in the order: rotating bending, alternating bending, pulsating bending. The fatigue life becomes shorter in proportion to the temperature rise.

(5) The fatigue limit of strain for alternating bending, pulsating bending and rotating bending is in the region of the R-phase transformation.

ACKNOWLEDGEMENTS

The experimental work for this study was carried out with the assistance of students in Aichi Institute of Technology, to whom the authors wish to express their gratitude. The authors also wish to extend thanks to Scientific Research (C) in Grants-in-Aid for Scientific Research by the Japan Society for the Promotion of Science for the financial support.

REFERENCES

[1] Funakubo, H. ed., *Shape Memory Alloys*, 1987, (Gordon and Breach Science Pub., New York).

[2] Sakuma, T., Iwata, U. and Kimura, Y., Cyclic behavior and fatigue life of TiNiCu shape memory alloy, *Fatigue '96*, 1996, 1, 173-178, (Pergamon).

[3] Holtz, R. L., Sadananda, K. and Iman, M. A., Fatigue thresholds of Ni-Ti alloy near the shape memory transition temperature, *Inter. J. Fatigue*, 1999, 21, S137-S145.

[4] Tobushi, H., Hachisuka, T., Hashimoto, T., and Yamada, S., Cyclic deformation and fatigue of a TiNi shape-memory alloy wire subjected to rotating bending, *Trans. ASME., J. Eng. Mater. Tech.*, 1998, 120, 64-70.

[5] Tobushi, H., Nakahara, T., Shimeno, Y. and Hashimoto, T., Low-cycle fatigue of TiNi shape memory alloy and formulation of fatigue life, *Trans. ASME, J. Eng. Mater. Tech.*, 2000, 122, 186-191.

[6] Gong, J. M., Tobushi, H., Takata, K. and Okumura, K., Superelastic deformation of a TiNi shape memory alloy subjected to various cyclic loadings, *Proc. Instn. Mech. Engrs., Part L, J. Mater. :Design & Appl.*, 2002, 216, 17-23.

[7] Tanaka, K., Kobayashi, S. and Sato, Y., Thermomechanics of transformation pseudoelasticity and shape memory effect in alloys, *Inter. J. Plasticity*, 1986, 2, 59-72.

(Received December 21, 2002; Accepted Febuary 5, 2003)